Flux Uniformity and Spectral Reproduction in Solar Concentrators Using Secondary Optics

Ralf Leutz[a,*], Akio Suzuki[b], Atsushi Akisawa[a] and Takao Kashiwagi[a]
[a]Tokyo University of Agriculture and Technology, BASE,
2-24-16 Naka-cho, Koganei-shi, Tokyo 184-8588, Japan
[b]UNESCO Natural Sciences Sector, 1 rue Miollis, 75732 Paris Cedex 15, France

Abstract

The design quality of the optical elements in a solar photovoltaic concentrator are the key to enable the exploitation of the efficiency potentials of multijunction devices. The cells require homogeneous flux over the cell area and reproduction of the solar spectrum, for which the thickness of the layers was designed. We discuss the possible efficiency impact of inhomogeneous flux. To solve the problems, we propose the use of a kaleidoskope-based secondary concentrators to achieve a uniform flux distribution and the reproduction of the spectrum of the incoming light. The (imperfect) design procedures of lens-based secondaries with the edge-ray principle are followed up.

Keywords: Dielectric total internal reflecting concentrator (DTIRC), flux uniformity, kaleidoscope-based homogenizer, nonimaging concentration, photovoltaic concentrator system

1 INTRODUCTION

Multijunction devices are promising the realization of solar photovoltaic power conversion with efficiencies $> 30\,\%$. These systems will only be successful if concentration is employed; multijunction cells are too expensive to be used under one sun (1000 W at 25℃) of irradiation, and there is a marginal increase of cell performance with increased radiation. While the short-circuit (maxium) current generated in a photovoltaic cell increases linearly with the concentration C,

$$I_{\rm sc} = C I_{{\rm sc}_0} \ , \tag{1}$$

the open-circuit voltage increases logarithmically as

$$V_{\rm oc} = V_{{\rm oc}_0} + n V_{\rm th} \ln(C) \ , \tag{2}$$

where n is a diode factor, and $nV_{\rm th}$ expresses the thermal dependency of the cell efficiency.

Multijunction cells can be designed for any level of concentration, provided the irradiance on the cell is homogeneous both in quantity and quality, i.e. locally evenly distributed and accurately reproducing the solar design spectrum.

There is notable progress in the development of multijunction cells, but solar concentrator optics sometimes appear to be taken less seriously, even though the optical components of a solar photovoltaic system are crucial for its successful operation. Three books are dealing specifically with photovoltaics and concentration: Luque [1989] edited an expensive standard work focussing on nonimaging optics and photovoltaic cell design issues. Andreev et al. [1997] describe the complexity of photovoltaic power conversion under concentration. Two authors of the present paper delivered their own account of nonimaging concentration in an application for photovoltaics in Leutz and Suzuki [2001]. As in the book, we are here lead by the notion that flux homogenuity, both in local density and spectral reproduction, will be the driving force behind the development of all future refractive concentrators for photovoltaic applications.

*Send correspondence to Ralf Leutz, ralfsun@cc.tuat.ac.jp (ralfsun@yahoo.com), phone/fax +81-42-388-7226; http://www.geocities.com/ralfsun

2 IRRADATION AND MULTIJUNCTION DEVICES

In this section we discuss theoretical aspects of flux inhomogenity on multijunction devices, and then turn to simulated and measured effects on the efficiency of the device.

2.1 Flux Homogenity

Multijunction photovoltaic cells are used with medium and highly concentrated sunlight. The conversion efficiency of concentrator cells increases with the concentration ratio, but the fill factor is degraded by increasing resistance losses. For state-of-the-art multijunction cells in concentrator systems, the flux characteristics of the concentrated sunlight must be accurately controlled to ensure optimum performance. The irradiation over the cell area should be kept constant.

Color effects, or the spectral mismatch between the cells in the multijunction device, can be expressed by a rule of thumb: if the spectral mismatch between cells in a multijunction device amounts to 20%, the total performance of the device is cut by 10% [Kurtz and O'Neill, 1996].

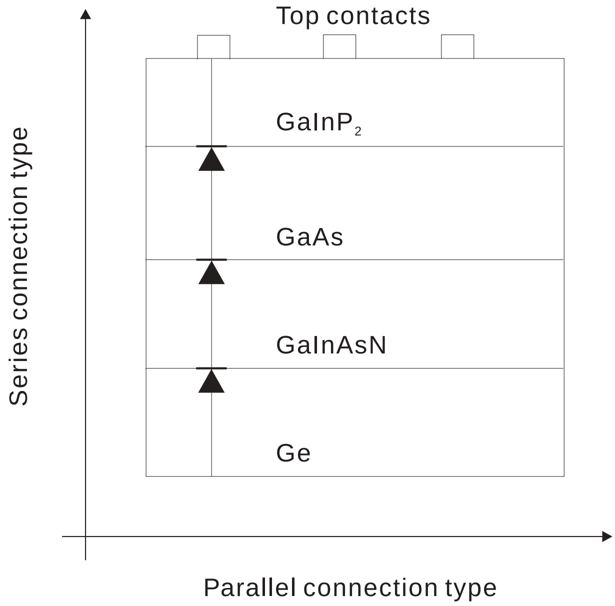

Figure 1: Typical multijunction photovoltaic concentrator device. For an explanation of the axis see text. Not to scale

Two forms of nonuniform illumination can be distinguished for the purpose of evaluating their influence on the performance of a multijunction cell; we distinguish quantitative and qualitative flux distributions.

The nonuniformly illuminated multijunction device can be approximated as a parallel connection of cells, where the total output current is the sum of cell components [Araki and Yamaguchi, 2000]. Partial illumination with medium and high concentration ratios causes distributed diode effects manifested in a degradation of the fill factor due to rounding of the I–V characteristics near the maximum power point [Araki et al., 2000]. For a typical multijunction cell, pictured schematically in Fig. 1, this type of inhomogeneous flux density is referred to as the 'parallel connection' type. One may also speak of the necessity to quantiatively ensure flux uniformity over the area of the device.

Multijunction cells additionally require color uniformity within area segments. Uniform color is defined here as the proportionality of band gaps, for which the cells have been designed, usually according to the direct normal solar spectrum. The thickness of each layer is designed so that each junction produces the same photocurrent [Kurtz et al., 1997]. Should the design spectrum change, as in the case of nonuniform color flux, one or more junctions will operate suboptimally, and limit the output of the cell, which is understood as being formed by junctions connected in series (Fig. 1). This type of inhomogeneous color flux shall be called the 'series connection' type. The efficiency reduction of the device is due to the quality of the reproduced spectrum.

The two types, parallel and series, should be separately treated in their effects on the cells, if the concentrator happens to be a Fresnel lens, or other refractive or dispersive concentrator. For reflective concentrators (mirrors), there is virtually no color dispersion, and the 'series connection' type ideally does not exist.

Solar spectral reproduction can be problematic for the optimum performance of a photovoltaic multijunction device. Possible solutions include the following [Leutz and Suzuki, 2001]:

- The redesign of the nonimaging lens: in theory, the nonimaging lens can be designed to produce uniform flux. The argument is that the degree of freedom remaining between the ideal theoretical lens with its uniform flux and the nonideal practical lens could be used to create a lens with prescribed flux distribution. Related work is under way by several researchers.
- The movement of the absorber closer to the lens or further away from it: A closer absorber performs marginally better in terms of color reproduction, but the absorber misses increase. In the case of the absorber being further away from the lens, less absorber misses are recorded, but worse color reproduction is observed. For an absorber located at $1.05f$, color reproduction at the center of the flux is quite good, while the system becomes more sensitive to incidence angles off normal, and flux uniformity over the absorber is strongly reduced, showing a strong peak.
- The placement of a reflective or refractive secondary concentrator in place of the original receiver: the secondary concentrator is called a homogenizer if the aim is to control the flux adding little or no geometrical concentration. The homogenizer can be an option to redirect rays and make the color flux more uniform, but first-order reflection losses at the secondary are substantial, and may exceed the losses caused by inhomogeneous flux. For their practical importance, the design and performance of secondaries will be more closely studied in the second half of this paper.
- The design of photovoltaic cells: instead of the redesign of the concentrator, the layers of the multijunction device could be designed and assembled with varying thickness according to the spectral fraction incident at that point. This may not be practical, since the angle of incidence of the radiation on the concentrator has a strong influence on the flux distribution at the absorber. Still, multijunction devices which are to be used with refractive solar concentrators must be designed for the flux and spectral reproduction the lens produces, i.e. the spectral transmittance of the lens material is a design parameter.

These measures not only complicate the design of the concentrator, but may also carry the risk of lower performance at incidence angles off normal. Careful analysis and design are necessary.

2.2 Spectral Mismatch

Other authors described the problem of color nonuniformity. Early descriptions are found in James and Williams [1978] and Moon et al. [1978]. Papers including a quantification of the chromatic aberration losses for multijunction cells are [James, 1994] (with imaging lenses), and [Kurtz et al., 1994, Kurtz and O'Neill, 1996] (with O'Neill's lens of medium concentration). The consensus seems to be that losses due to color dispersion are smaller than other losses, and that they may be controlled by design measures such as resistance and diode quality. Still, for testing and operating high-performance cells, the color behavior of the optical system must be well understood. For advanced multi-junction cells color aberrations may prove to be second in importance for the devices' efficiencies only to tracking errors.

Kurtz and O'Neill [1996] mention 4% losses due to chromatic aberrations, if the system was aligned optimally. For less optimum cases, they predict a performance loss of the device by 10%, if the spectral mismatch between cells in a multijunction device amounts to 20%. Our simulations show that refractive concentrator systems are very sensitive when spectral changes in the flux distrbution could be incurred. Color behavior will be of concern for practical systems, more so than for laboratory tests. Testing of multijunction cells is performed in controlled surroundings, where the image is larger than the cell. Such overdimensioning of the concentrator system leads to more uniform flux over the area of a small cell, but to losses unacceptable in practical applications.

In their model, Araki and Yamaguchi calculate the non-linear response of concentrator cells to chromatic aberrations. The latter are calculated as cosine distributions of three wavelength ranges related to the three junctions of a III/IV-device, and superimposed on the Gaussian flux distribution of a real concentrator. Like in [Kurtz and O'Neill, 1996] chromatic aberrations are measured in per cent, but

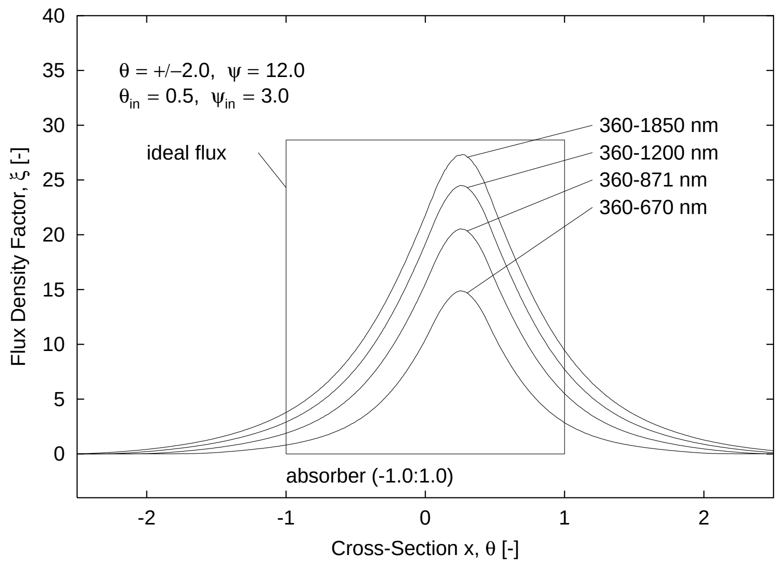

Figure 2: Solar spectral flux reproduction of the nonimaging linear Fresnel lens; design acceptance half angles θ and ψ in degree, incidence in the cross-sectional plane $\theta_{\rm in}$, and in the plane of the paper $\psi_{\rm in}$. Reasons for the difference between ideal and simulated spectral flux include the finite refractive index of the lens, and truncation of the lens

the work of Kurtz and O'Neill is extended for high concentrations, including a dynamic behavior of the diode. Results confirm the importance of chromatic aberrations, and indicate that losses of 30% are to be expected once the chromatic flux distribution on the multi-junction device differs from the design spectrum by 50%.

3 SECONDARY CONCENTRATORS

Secondary optics in the solar concentrator offer possibilities of

- increasing the concentration ratio;
- homogenizing the flux over the with of the absorber quantitatively; and
- correcting chromatic aberration in the reproduction of the solar spectrum, e.g. homogenizing the flux in a qualitative way.

This is achieved at the cost of higher optical losses. For every surface the ray passes by refraction or reflection on its way from the entry aperture to the exit aperture of the optical system, some 5% additional losses should be included in a rough calculation of the optical efficiency of the concentrator. The following two subsections deal with simple kaleidoscopic mirrors for flux homogenization, and with dielectric total internal reflection concentrators (DTIRC) as more complicated means to achieve both concentration and flux uniformity.

3.1 Kaleidoscope Flux Homogenizer

A typical reproduction of the solar spectrum by an existing nonimaging device, a linear Fresnel lens, is shown in Fig. 2. Clearly, both the local irradiance is changing over the locations over the absorber, and the solar spectrum is not equally reproduced for all locations. The latter is indicated by the relative changes in the vertical distance between the graphs representing cumulative energy for response ranges for light of various wavelengths. Optimum performance of the solar cell can only be expected under ideal flux (Fig. 2). Flux issues, such as the simulation method have been discussed elsewhere [Leutz and Suzuki, 2001, Leutz et al., 2000].

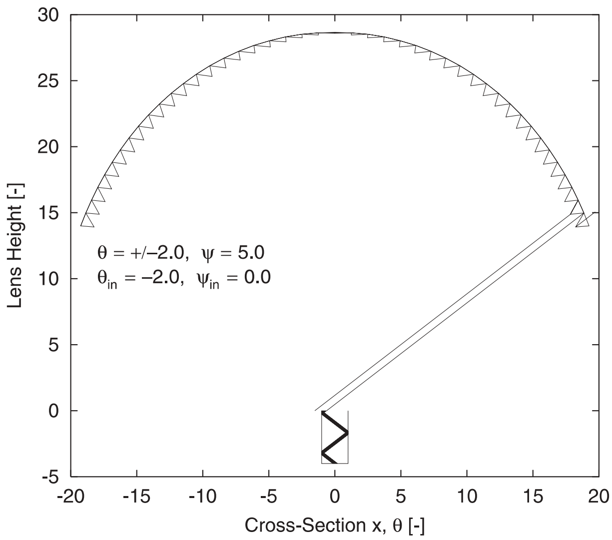

Figure 3: Nonimaging Fresnel lens with kaleidoskope diffusor; ray tracing for one ray bundle incident at $\theta_{\rm in} = -2.0$ degrees from the right, and $\psi_{\rm in} = 0.0$ out of the plane of the paper. The lens has design acceptance half angles of θ and ψ

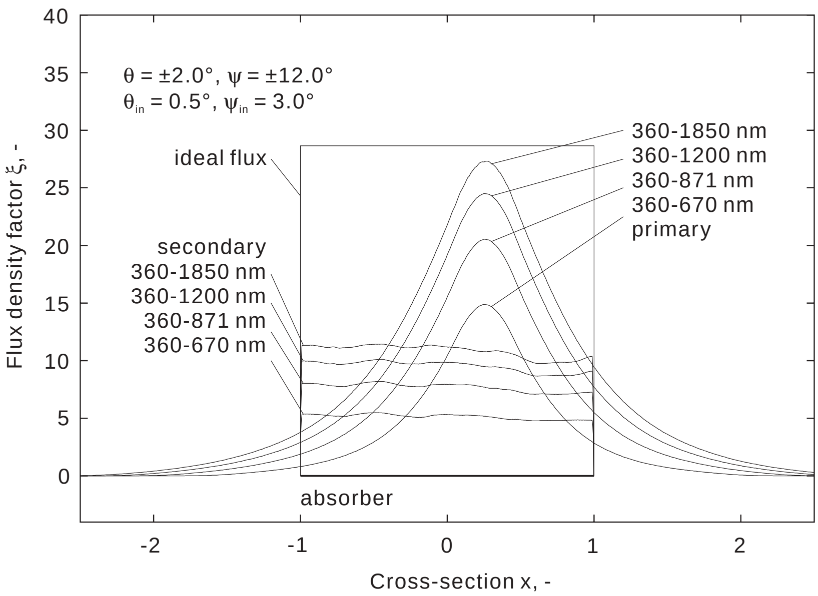

Figure 4: Color flux density factors and solar spectral reproduction for the nonimaging Fresnel lens of acceptance half-angle pairs $\theta = \pm 2°$ and $\psi = \pm 12°$ with and without secondary kaleidoskope-based homogenizer. Incidence away from the normal by $\theta_{\rm in} = 0.5°$ and $\psi_{\rm in} = 3.0°$. Depth of the secondary $12.6\,d$

A kaleidoskope-based secondary homogenizer [Chen et al., 1963, Ries et al., 1997a] for the linear lens can be constructed from two parallel mirrors forming a trough of absorber width under the original absorber level (Fig. 3). In the example given in Fig. 4 (inspired by J. Gordon), we use a secondary with a depth of $12.6\,d$, where d is the absorber half-width. Clearly, the flux uniformity and the reproduction of the solar spectrum improve. Additional reflection losses τ can be calculated with

$$\tau = \rho_{\rm m}^{\rm n} \,. \tag{3}$$

With (3), reflection losses at the mirror sides of the secondary are 9.8% using a reflectivity of the mirror $\rho_{\rm m} = 0.95$ and the average number of reflections $n = 2.01$. The effectiveness of the kaleidoskope-based secondary was confirmed in our experiment.

When a pair of kaleidoscope mirrors is used in analogy to Figs. 3 and 4, the flux over the absorber is quite uniform. This leads to an improved fill factor FF. Unfortunately, our preliminary experiments are conducted with silicon concentrator cells, not with multi-junction devices. Thus, we cannot deduct the important of the chromatic homogenization achieved by the kaleidoscope, but have to limit ourselves to describing that optical losses increased, in this case significantly stronger than the efficiency gain due to the improved fill factor.

This should tell us to stick with the long-known rule that flux inhomogenuity is of minor importance for the efficiency of single cells, such as silicon concentrator cells. Here, the amount of radiation incident on the cell (no matter where or in which wavelength) is the dominant factor.

The optics of concentrators for multi-junction cells, on the other hand, should be improved, since the simulations described show that the efficiency reduction, in particular the one due to chromatic aberrations are significant and several times higher than the additional losses encountered with secondary optics.

3.2 Dielectric Total Internal Reflection Concentrators

Dielectric total internal reflecting concentrators (DTIRC) have been developed in the group of Winston in Chigaco [Ning et al., 1987]. They are the result of nonimaging optical theory and take advantage of the optical properties of a dielectricum, namely its refractive index, which leads to total internal reflection. Snell's law of refraction explains the angle of refraction Ψ' of a ray entering an optical thicker medium with refractive index n' at an angle Ψ from an optically thinner medium with refractive index n:

$$\frac{\sin\Psi}{\sin\Psi'} = \frac{n'}{n} \ . \tag{4}$$

Should $n = 1.0$ be the refractive index of air surrounding the DTIRC, and the entering ray be incident at an angle of $\Psi = 90.0°$, equation (4), solved for Ψ' yields the critical angle, or angle of total internal reflection (TIR). The principle of the reversibility of light demands that rays reaching the interface between an optical thicker medium and the thinner medium surrounding it at an angle greater than the critical angle (always measured to the normal of the surface) must be reflected, and not refracted. This is total internal reflection. Its main advantage is that, contrary to common reflections at mirror surfaces, TIR is quite free of losses. Furthermore, the concentration ratio C of a device depends on the refractive index n of its material,

$$C_{2\mathrm{D}} = \frac{n}{\sin\theta} \ , \tag{5}$$

where θ is the acceptance half-angle of the linear nonimaging concentrator, including such devices as the DTIRC. Three-dimensional system, such as a DTIRC of rotational symmetry must be evaluated using the similarly well known

$$C_{3\mathrm{D}} = \frac{n^2}{\sin^2\theta} \ . \tag{6}$$

Practical DTIRC have two or three stages: a spherical (or aspherical, but this has not been done) convex lens surface; a conic section for further concentration; and, not compulsory, a third section for light transport or the like.

DTIRC can be ideal nonimaging devices [Ning et al., 1987] featuring tailored wall shapes, but for practical purposes may be designed with straight sides of the conic section. A illustrative example which provided us with most of the equations used in our designs is found in Soules et al. [1997]. Starting from the one example calculated there, we distinguish four types of DTIRC clones as shown in Fig. 5.

- n-DTIRC close to the nonimaging optium; two stages, lens and cone; straight walls (for the real optimum with parabolic or hyperbolic side walls see Ning et al. [1987]); the design criterion is a an exit angle of 90°;
- e-DTIRC with extractor, meaning that the flux will only exit the third stage of the secondary, if a flux extractor is provided (see Ries et al. [1997b]); the design maintains total internal reflection at the side walls of the extractor; this is the design presented in Soules et al. [1997];

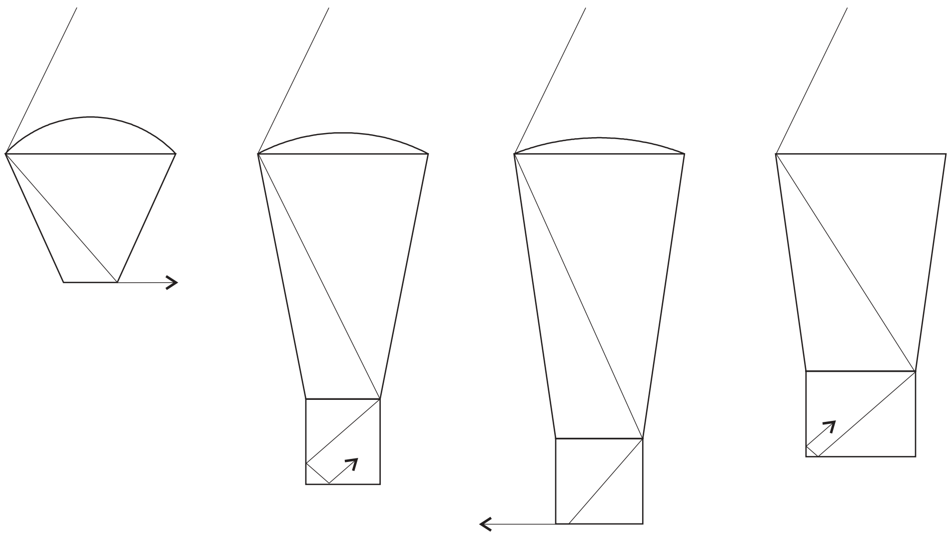

Figure 5: Dielectric total internal reflection concentrators (DTIRC). The DTIRC have a design acceptance half angles of $\theta = \pm 26°$, their apertures are unity to illustrate the differences in concentration ratio and size. Shown is one edge-ray for each clone. Material of the DTIRC is BK7 glass, with $n_{\mathrm{BK7}} = 1.52$; surrounded by air with $n_{\mathrm{air}} = 1.0$

- h-DTIRC with homogenizer; here the flux will exit the flat bottom of the third stage of the device, even if the index of refraction of the surrounding medium is unity, the design equals the n-DTIRC but allows for a homogenizer (which must not be round, but must be triangular, rectangular, or octagonal [Ries et al., 1997a]);
- v-DTIRC with concave first stage; actually the first stage is flat, as the radius of the singlet converges to infinity in the simulation, which focuses on maxium concentration; again, the system is designed with extractor.

Clearly, the length of the devices varies, as do their geometrical concentration ratios, which are for linear devices $C_{\mathrm{n}} = 3.17$, $C_{\mathrm{e}} = 2.30$, $C_{\mathrm{h}} = 1.96$, $C_{\mathrm{v}} = 1.56$, while the ideal concentration ratio defined by equation (5) yields $C_{\mathrm{2D}} = 3.46$.

When tracing rays incident at the design (acceptance half-) angle $\theta = 26°$ in Figs. 6-9, we find that the straight wall version of the ideal n-DTIRC leads to losses. While the edge-ray follows the design criterion, some of the neighboring rays exit the side wall of the device. In order for the nonimaging concentrator to be called ideal, the edge-rays at the entry aperture must be the edge-rays at the exit aperture, which they are not.

Apparently a violation of the edge-ray principle, the problem must be attributed to the limitations of being restricted to use straight walls and a spherical surfce lens. Relaxing either solves the isseu: DTIRC with shaped walls [Ning et al., 1987] reach ideal concentration. If the lens surface is to be aspherically tailored with the optical path length method, the same goal should be obtainable.

This example shows that te edge-ray principle is a necessary tool for the design of nonimaging devices, but that its employment is not sufficient to generate ideal concentrators. Apart from the n-DTIRC, all other clones work as designed, nowhere near the limit of concentration, but fulfilling their design purposes.

For the purpose of our study, the h-DTIRC has been designed as concentrator and homogenizer for photovoltaic concentration. The homogenizer directs the light towards the secondary's bottom where the rays exit, even if the refractive index of the surrounding medium is as low as the one of air. The refractive index of a photovoltaic cell may be in the range of 2-6, which would allow a design closer to the characteristics of the e-DTIRC, with higher concentration ratio, as the change of the critical angle may allow the ray to exit through the bottom of the secondary.

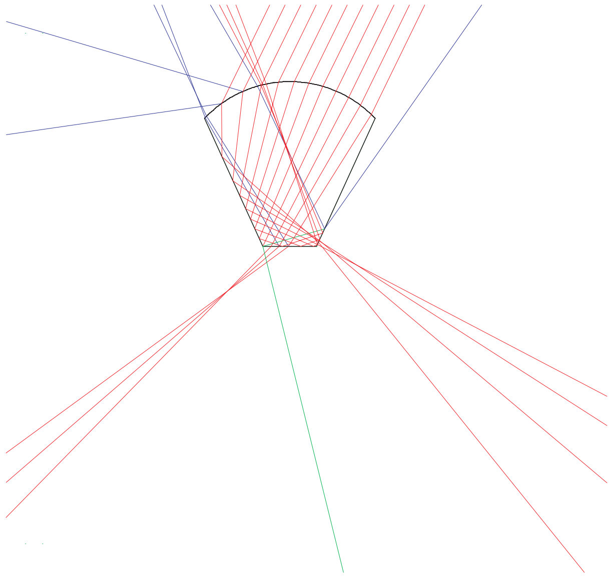

Figure 6: Ray tracing of the n-DTIRC with acceptance half angle of $\theta = \pm 26°$ and $n_{\mathrm{BK7}} = 1.52$ surrounded by air with $n_{\mathrm{air}} = 1.0$

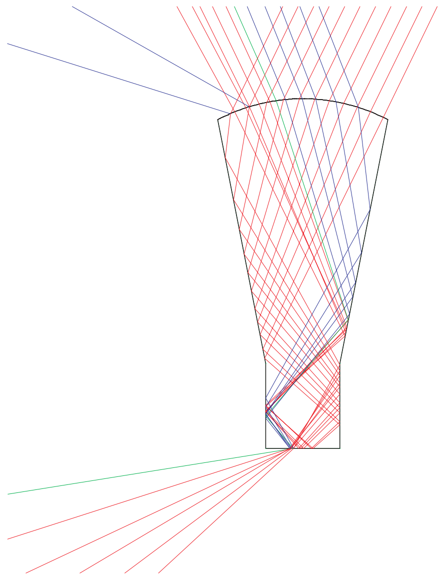

Figure 7: Ray tracing of the e-DTIRC with acceptance half angle of $\theta = \pm 26°$ and $n_{\mathrm{BK7}} = 1.52$ surrounded by air with $n_{\mathrm{air}} = 1.0$

The dielectric concentrators pictured here are linear two-dimensional models, and not of three-dimensional rotational symmetry. In the latter case, the problem of skew rays arises, i.e. rays which are not lying in any plane which also contains the optical axis of the system. Others [Luque, 1989] have argued that over-designing the concentrator can solve the problem; namely by setting the acceptance half-angle a few degrees wider than the angle of incidence expected. In respect of the n-DTIRC above, we support this notion, and require ray tracing before employing three-dimensional DTIRC.

3.3 DTIRC Designs

As mentioned above, the principle behind the design of DTIRC is most completely described in Soules et al. [1997]. The design follows the edge-ray principle of nonimaging optics, which states that in order to be called ideal the edge-rays at the entry aperture must be the edge-rays at the exit aperture. This is a necessary principle; it is not sufficient, as can be seen in the nonideal example in Fig. 6.

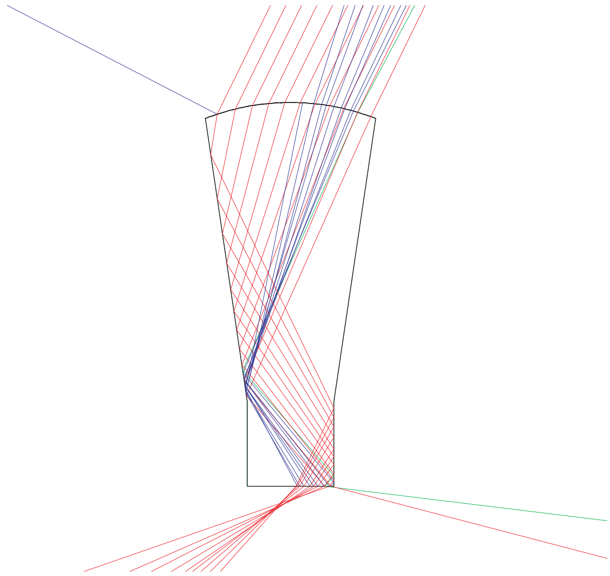

Figure 8: Ray tracing of the h-DTIRC with acceptance half angle of $\theta = \pm 26^\circ$ and $n_{\mathrm{BK7}} = 1.52$ surrounded by air with $n_{\mathrm{air}} = 1.0$

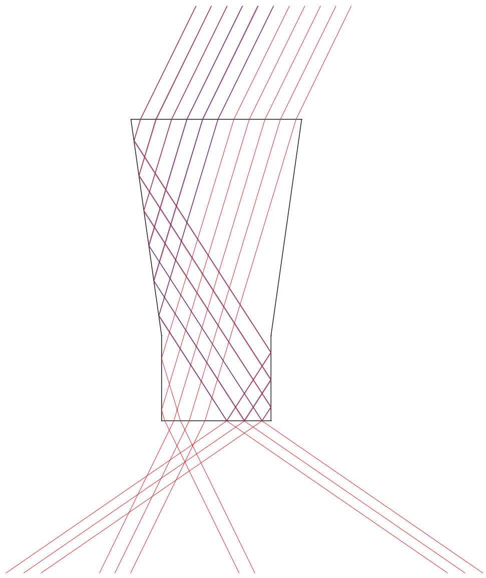

Figure 9: Ray tracing of the v-DTIRC with acceptance half angle of $\theta = \pm 26^\circ$ and $n_{\mathrm{BK7}} = 1.52$ surrounded by air with $n_{\mathrm{air}} = 1.0$

Although the design solution for an ideal DTIRC can have an analytical solution [Ning et al., 1987], our designs are found numerically, if in a simple way. The design (Fig. fig:dtircnom) works by defining a pair of acceptance half-angles θ for the system, thereby stating its ideal concentration ratio following equation (5). The next step is central to the numerical nature of the calculation: a relation between the width of the system and the radius of the convex or concave surface of the DTIRC is established.

$$\gamma = \arcsin\left(\frac{d}{2r}\right) . \tag{7}$$

The design now is following two paths, one for the left edge-ray, one for the right edge-ray as shown in Fig. fig:dtircnom. The angles within the cone section are found analytical, except in our version of the v-DTIRC where the angle Δ is found by a second application of Newton's method, which serves as

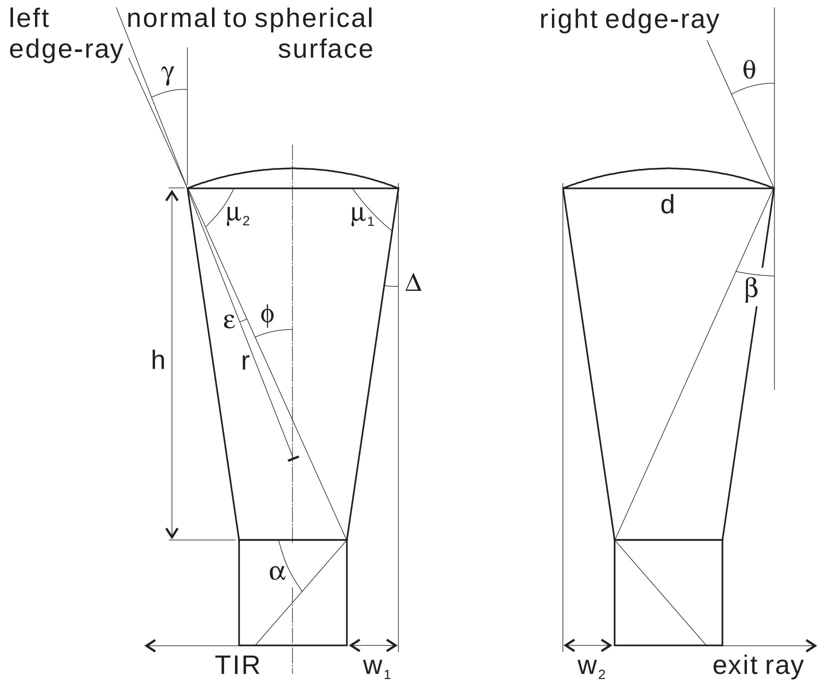

Figure 10: Nomenclature for the design of a dielectric total internal reflection concentrator with homogenizer (h-DTIRC)

numerical tool for solving the relation (7). For the typical case, for the left edge-ray:

$$\varepsilon = \arcsin\left(\frac{\sin(\theta-\gamma)}{n}\right) , \quad (8)$$

$$\phi = \gamma + \varepsilon , \quad (9)$$

$$\Delta = \frac{90-\alpha-\phi}{2} , \quad (10)$$

$$\alpha = f\,(\text{condition}) , \quad (11)$$

$$\mu_1 = 90 - \Delta , \quad (12)$$

$$\mu_2 = 90 - \phi , \quad (13)$$

$$h = d\frac{\sin\mu_1 \sin\mu_2}{\sin(\mu_1+\mu_2)} , \quad (14)$$

$$w_1 = h\tan\Delta . \quad (15)$$

The condition in (11) defines the design. For the e-DTIRC and the v-DTIRC, $\alpha = \arcsin(1/n)$, the design asking for total internal reflection at the side walls of the third stage. For the h-DTIRC, this condition changes to $\alpha = 90 - \arcsin(1/n)$, the complimentary angle to the TIR-angle, because the requirement is that radation must exit the third stage at the bottom.

For the ideal DTIRC, there is no third stage, and the condition is moved upwards, stating that $\phi = \arcsin(1/n)$.

The definition of the right edge-ray is simpler, using the same equation as for the left edge-ray, except the following:

$$\varepsilon = \arcsin\left(\frac{\sin(\theta+\gamma)}{n}\right) , \quad (16)$$

$$\beta = \varepsilon - \gamma + 2\Delta , \quad (17)$$

$$w_2 = d - h\tan\beta . \quad (18)$$

The numerical solution searches for a value for the radius r, for which the lengths w_1 and w_2 are equal (their difference zero). This ensures the symmetry of the system. For a similar example on the embedding of Newton's method in an infinity loop when implementing the problem into computing code, see Leutz and Suzuki [2001].

The setup of the problem requires a positive concentration ratio as outcome. In the case of the v-DTIRC, positive concentration cannot be achieved with a concave surface. Accordingly, the value for the radius of the lens in this case $r \to \infty$.

4 CONCLUSIONS

The aim of this paper was to identify color flux uniformity as the main driving force behind the development of future solar concentrator optics for multi-junction cells. We hoped to clarify the theoretical role of color aberrations as qualitative flux problem as opposed to the quantitative local distribution of flux.

These considerations lead to the necessity of secondary optics for advanced concentrators, if flux homogenity is not achievable by the appropriate design of the primary. The simple kaleidoscope mirror is a suitable tool achieving uniform flux distribution. Additional concentration is desirable for high-quality concentrator systems, and one may take advantage of the few losses offered by dielectric concentrators with total internal reflection (DTIRC). These are relatively simple to design and offer good performance. The design procedures for four DTIRC clones are presented to illuminate the underlying assumptions, in particular the powerful role of the edge-ray principle as design tool in nonimaging optics which is not sufficient to create ideal concentrators. We would like to insist on the design of special optics for each case of solar concentration.

ACKNOWLEDGEMENTS

We would like to thank K. Araki of the Toyota Technological Institute for sharing the results of his work on the simulation of color mismatching in multijunction devices, and for fruitful discussions. K. Komai has skillfully conducted 'our' experiments.

References

V.M. Andreev, V.A. Grilikhes, and V.D. Rumyantsev. *Photovoltaic Conversion of Concentrated Sunlight.* Wiley, Chichester, 1997.

K. Araki and M. Yamaguchi. Extended distributed model for analysis of non-ideal concentration operation. *Solar Energy Materials and Solar Cells.* To be published.

K. Araki, M. Yamaguchi, M. Imaizumi, S. Matsuda, T. Takamoto, and H. Kurita. AM0 concentration operation of III–IV compound solar cells. In *Proceedings of the 28th IEEE Photovoltaic Specialists Conference*, Anchorage, Alaska, September 2000.

K. Araki and Y. Yamaguchi. Parameter analysis on solar concentrator cells under nonuniform illumination. In *16th European Photovoltaic Conference and Exhibition*, Glasgow, United Kingdom, May 2000.

M.M. Chen, J.B. Berkowitz-Mattuck, and P.E. Glaser. The use of a kaleidoskope to obtain uniform flux over a large area in a solar or arc imaging furnace. *Applied Optics*, 2(3):265–271, 1963.

L.W. James. Effects of concentrator chromatic aberration on multi-junction cells. In *Proceedings of the 1994 IEEE First World Conference on Photovoltaic Energy Conversion, and the 24th IEEE Photovoltaic Specialists Conference*, pages 1799–1802, Waikoloa, Hawaii, December 1994.

L.W. James and J.K. Williams. Fresnel optics for solar concentration on photovoltaic cells. In *Proceedings of the 13th IEEE Photovoltaic Specialists Conference*, pages 673–679, 1978.

S.R. Kurtz, D.J. Friedman, and J.M. Olson. The effect of chromatic aberrations on two-junction, two-terminal devices in a concentrator system. In *Proceedings of the 1994 IEEE First World Conference on Photovoltaic Energy Conversion, and the 24th IEEE Photovoltaic Specialists Conference*, Waikoloa, Hawaii, December 1994.

S.R. Kurtz, D. Myers, and J.M. Olson. Projected performance of three- and four-junction devices using GaAs and GaInP. In *Proceedings of the 26th IEEE Photovoltaic Specialists Conference*, Anaheim, California, September 1997.

S.R. Kurtz and M.J. O'Neill. Estimating and controlling chromatic aberration losses for two-junction, two-terminal devices in refractive concentrator systems. In *Proceedings of the 25th IEEE Photovoltaic Specialists Conference*, pages 361–364, Washington, D.C., May 1996.

R. Leutz and A. Suzuki. *Nonimaging Fresnel Lenses: Design and Performance of Solar Concentrators.* Springer Verlag, Heidelberg, July 2001.

R. Leutz, A. Suzuki, A. Akisawa, and T. Kashiwagi. Flux densities in optimum nonimaging Fresnel lens concentrators for space. In *Proceedings 28th IEEE Photovoltaic Specialists Conference*, Anchorage, Alaska, September 2000.

A. Luque. *Solar Cells and Optics for Photovoltaic Concentration.* Adam Hilger, Bristol, 1989. With contributions of G.L. Araújo, A. Cuevas, E. Lorenzo, J.C. Miñano, J.M. Ruiz and G. Sala.

R.L. Moon, L.W. James, H.A. Vander Plas, T.O. Yep, G.A. Antypas, and Y. Chai. Multigap solar cell requirements and the performance of AlGaAs and Si cells in concentrated sunlight. In *Proceedings of the 13th IEEE Photovoltaic Specialists Conference*, pages 859–867, 1978.

X. Ning, R. Winston, and J. O'Gallagher. Dielectric totally internally reflecting concentrators. *Applied Optics*, 26(2):300–305, 1987.

H. Ries, J.M. Gordon, and M. Lasken. High-flux photovoltaic solar concentrators with kaleidoskope-based optical designs. *Solar Energy*, 60(1):11–16, 1997a.

H. Ries, A. Segal, and J. Karni. Extracting concentrated guided light. *Applied Optics*, 36(13):2869–2874, 1997b.

J.A. Soules, D.R. Buchele, C.H. Castle, and R.P. Macosko. Design and fabrication of a dielectric total internal reflecting solar concentrator and associated flux extractor for extreme high temperature (2500k) applications. NASA contract report 204145, National Aeronautics and Space Administration (NASA), Lewis Research Center, Cleveland, Ohio 44135-3191, November 1997. ftp://ftp-letrs.lerc.nasa.gov/LeTRS/reports/1997/CR-204145.pdf.